ARTICLE
PUBLISHED ONLINE: 3 JULY 2017 | DOI: 10.1038/NCHEMBIO.2418

nature chemical biology

A molecular rheostat maintains ATP levels to drive a synthetic biochemistry system

Paul H Opgenorth, Tyler P Korman, Liviu Iancu & James U Bowie*

Synthetic biochemistry seeks to engineer complex metabolic pathways for chemical conversions outside the constraints of the cell. Establishment of effective and flexible cell-free systems requires the development of simple systems to replace the intricate regulatory mechanisms that exist in cells for maintaining high-energy cofactor balance. Here we describe a simple rheostat that regulates ATP levels by controlling the flow down either an ATP-generating or non-ATP-generating pathway according to the free-phosphate concentration. We implemented this concept for the production of isobutanol from glucose. The rheostat maintains adequate ATP concentrations even in the presence of ATPase contamination. The final system including the rheostat produced 24.1 ± 1.8 g/L of isobutanol from glucose in 91% theoretical yield with an initial productivity of 1.3 g/L/h. The molecular rheostat concept can be used in the design of continuously operating, self-sustaining synthetic biochemistry systems.

Over the past few decades, there has been a keen interest in engineering cellular metabolism for the production of green chemicals that could wean us off of our reliance on petrochemicals[1]. However, cellular engineering efforts to date have had limited success because of difficulties in obtaining the high yields, high productivity and high titers needed for the economic competitiveness of low-value chemicals such as biofuels. The shortcomings of cellular engineering are mainly due to the complexities of cellular metabolism and constraints imposed by having to maintain cell viability[2]. Although considerable progress has been made to address these challenges, it may also be reasonable to consider different approaches.

An alternative approach to bio-based chemical manufacturing seeks to free us from the constraints of cells by performing the desired biochemical conversions using purified enzymes or cell-free extracts[3–9]. Cell-free metabolic systems have many potential advantages over *in vivo* efforts, including continuous product production, ease of product removal, near-100% yields and lack of cell toxicity issues[10–14]. However, building cell-free pathways that can economically sustain high flux for long periods of time without the metabolic regulatory systems that exist in cells requires new design principles—a field we refer to as synthetic biochemistry.

A key consideration in synthetic biochemistry system design is the generation, regulation and recycling of high-energy cofactors such as ATP, NADH and NADPH. Generally, high-energy cofactors are generated in a catabolic or breakdown phase (for example, glycolysis), then used and regenerated in an anabolic or biosynthetic phase in which the desired chemicals are constructed[8,15]. The simplest way to design synthetic biochemistry systems is to demand perfect stoichiometry, i.e., that if two ATP are generated in the breakdown phase, then two ATP are used in the biosynthetic phase. Stoichiometric systems can allow flux through the pathway for a period of time, but the second law of thermodynamics dictates that flux will eventually decrease as ATP is hydrolyzed or NADH is oxidized spontaneously or by undesired side reactions. Ideally, we would like to design systems that can restore levels of high-energy cofactors as they become depleted over time. In prior work we described a molecular purge valve system that can maintain high NADPH levels to drive synthetic biochemistry systems[16,17]. Here we introduce a simple rheostat node for the maintenance of ATP levels.

As a proof of concept, we tested rheostat's ability to maintain ATP and improve isobutanol production in a cell-free system. Isobutanol is a desirable next-generation biofuel and commodity chemical. It has been produced in a variety of cellular systems[18–20], and represents perhaps the greatest metabolic-engineering success story. *Escherichia coli* has been engineered to produce isobutanol at 23 g/L, with titers exceeding 50 g/L when gas stripping is performed to remove isobutanol during production to reduce toxicity[21]. Isobutanol has also been produced from glucose in a clever cell-free system, although its final titers were substantially lower (0.76 g/L)[15]. Here we describe a new cell-free enzymatic pathway implementing a molecular rheostat that produces 24.1 ± 1.8 g/L of isobutanol from glucose at 91.5% theoretical yield over 48 h, already exceeding parameters seen for one of the best cell-based production systems reported to date[18–21]. This cell-free pathway also further illustrates the potential of the synthetic biochemistry approach for making bio-based chemicals.

RESULTS

A stoichiometric isobutanol pathway

We first designed and implemented a pathway to make isobutanol with stoichiometric recycling of high-energy cofactors (**Fig. 1a**) before implementing a rheostat-using pathway (**Fig. 1b**,**c**). The 2-ketoacid isobutanol biosynthetic phase employs two equivalents of pyruvate and two equivalents of NADPH, but no ATP, whereas the canonical glycolysis pathway produces two equivalents each of pyruvate, NADH and ATP. Thus, to make the cofactor use stoichiometric, we needed to generate two equivalents of NADPH instead of NADH and also eliminate net ATP production. With these constraints in mind, we designed the 14-enzyme pathway shown in **Figure 1a** (more detail shown in **Supplementary Results**, **Supplementary Fig. 1**), in which glyceraldehyde phosphate dehydrogenase (GapDH) and phosphoglycerate kinase (PGK) are replaced with a nonphosphorylating glyceraldehyde phosphate dehydrogenase (GapN). The use of GapN eliminates the production of two ATP equivalents and generates NADPH rather than NADH[22]. The overall pathway thus becomes stoichiometric with respect to the production and consumption of both ATP and NADPH.

We first modeled the overall pathway shown in **Figure 1a** using COPASI[23] to identify likely key steps in the pathway. The model

Department of Chemistry and Biochemistry, UCLA-DOE Institute for Genomics and Proteomics, Molecular Biology Institute, University of California, Los Angeles, Los Angeles, California, USA. *e-mail: bowie@mbi.ucla.edu

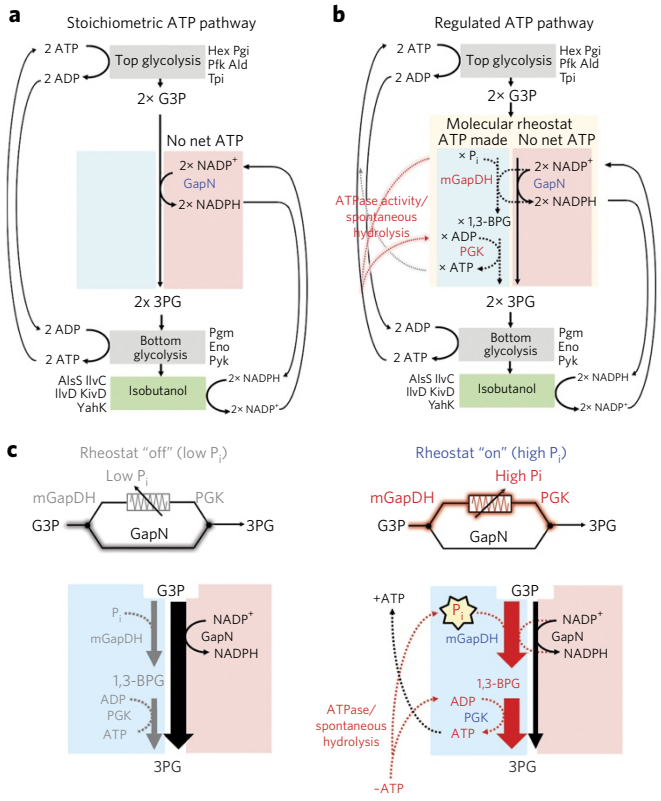

Figure 1 | Pathway designs for converting glucose to isobutanol. (**a**) Schematic of the stoichiometric pathway, in which there is no net ATP production and NADPH production and utilization are completely balanced. (**b**) Schematic of the synthetic biochemistry pathway with the 'molecular rheostat'. Enzymes mGapDH and PGK scavenge P_i to restore ATP that has been hydrolyzed in the system. (**c**) Schematic of the operation of the molecular rheostat. At low P_i concentrations (high-energy γ-phosphate (i.e., ATP) levels are high), the GapN pathway is preferred, generating no additional ATP. At high P_i concentrations (loss of high-energy γ-phosphate, resulting in low levels of ATP), the mGapDH–PGK pathway can be used to restore high-energy γ-phosphate to ATP. G3P, glyceraldehyde-3 phosphate; 3PG, 3-phosphoglycerate; 1,3-BPG, 1,3-bisphosphoglycerate.

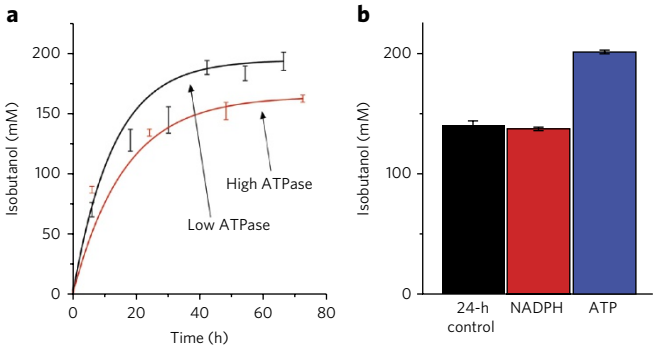

Figure 2 | Isobutanol production using the stoichiometric pathway. (**a**) Time course of isobutanol production from glucose by the stoichiometric pathway using a fully purified system. The initial time course (red) had a high amount of ATPase contamination and produced 11.96 ± 1.57 g/L. The second time course (black) had a lower amount of ATPase activity, which increased isobutanol production to 14.26 ± 0.57 g/L. (**b**) Histogram of isobutanol production from glucose by the stoichiometric pathway after 48 h upon NADPH or ATP supplementation at 24 h. Control, the same reaction without NADPH or ATP supplementation. Error bars represent the s.d. of biological replicates performed in triplicate.

revealed that the relative activities of hexokinase (Hex) and phosphofructokinase (Pfk) were critical for achieving flux through the system. This result is logical, because in glycolysis, Hex and Pfk compete with each other for any available ATP. Therefore, when the relative activity of Hex is too high, ATP can be rapidly exhausted in the production of glucose-6-phosphate (G6P), leaving insufficient ATP for the Pfk reaction and thereby stopping carbon flux. With this in mind, we set up initial reactions with Hex as the limiting enzyme. Once isobutanol production from glucose was detected, cofactor and enzyme concentrations were systematically optimized, resulting in the production time course shown in **Figure 2a**. The high initial productivity sharply decreased after 18 h, reaching a final titer of 161 ± 3 mM (11.9 ± 0.2 g/L) isobutanol after 3 d.

As the pathway is stoichiometrically balanced with respect to ATP production and consumption, we speculated that the sharp decrease in reaction rate might be due to ATPase activity contamination in the system. We therefore measured the ATPase activity of each of the individual enzymes in the pathway, and found that the enolase and IlvC enzyme preparations possessed notably higher ATPase levels than the other enzymes in the system. We therefore re-purified enolase and IlvC, which resulted in reduced contaminating ATPase activity. The stoichiometric reaction was set up again with the re-purified enzymes, leading to an improved titer of 192 ± 8 mM (14.2 ± 0.6 g/L) isobutanol over the course of 3 d. Nevertheless, isobutanol production still sharply decreased after 18 h.

We then tested whether cofactor depletion remained a problem by initiating the reactions as usual and then adding another bolus of ATP or NADPH after 24 h (**Fig. 2b**). After 48 h, the reaction supplemented with NADPH showed no change in isobutanol production, but the ATP-supplemented reaction showed a 41% increase of isobutanol production compared to the control that had no added bolus of cofactor. These results suggested that ATP hydrolysis, whether by ATPase contamination or spontaneous ATP hydrolysis, may have been the limiting factor for isobutanol production in this stoichiometric pathway even after multiple attempts to remove ATPase contamination. The ATPase activities present in all the enzyme preparations are listed in **Supplementary Table 1**.

Design of an ATP rheostat

The results described above suggested that ATP depletion was a major problem for the long-term sustainability of the stoichiometric reaction system. One way to deal with this problem might be to scrupulously purify all enzymes to eliminate any ATPase activity. However, even with total purity, it may never be possible to completely eliminate spontaneous hydrolysis or hydrolysis by imperfect kinase reactions. Moreover, requiring completely pristine enzyme preparations is impractical and expensive on a large scale. Thus, we sought to establish a method that could restore and regulate ATP levels as an intrinsic feature of the system. To this end, we designed a molecular rheostat.

Our molecular rheostat (**Fig. 1b,c**) is made up of two complementary pathway branches that both eventually transform glyceraldehyde-3 phosphate (G3P) into 3-phosphoglycerate (3PG). The main difference between the two branches is that one generates ATP whereas the other does not. Flow through the two branches is regulated by levels of ATP and inorganic phosphate (P_i). The first branch consists of one enzyme, the nonphosphorylating GapN, also used in the stoichiometric pathway, which reduces $NADP^+$ to NADPH and converts G3P directly into 3PG without generating ATP. The second branch is composed of two enzymes, an $NADP^+$-specific, phosphorylating G3P dehydrogenase (mGapDH) and PGK. This

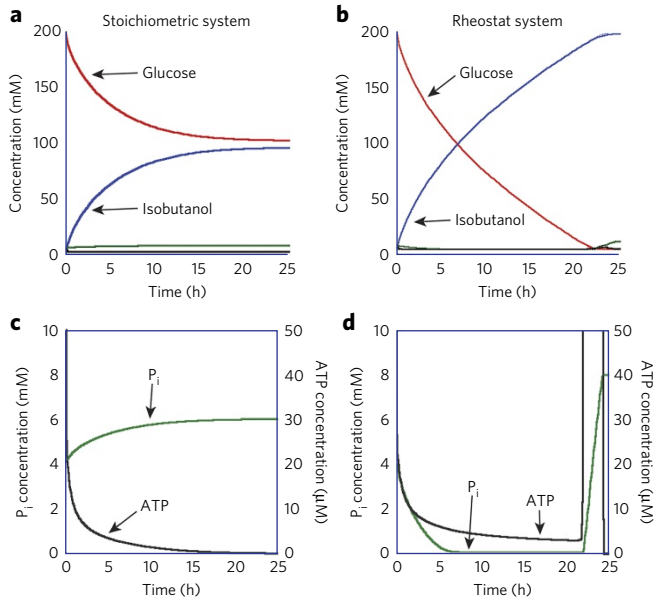

Figure 3 | Reaction modeling of isobutanol production by a system with or without the molecular rheostat in the presence of contaminating ATPase activity. (**a**) Glucose (red), isobutanol (blue), P_i (green) and ATP (black) levels over time in a model of the stoichiometric pathway including ATPase activity. (**b**) Glucose, isobutanol, P_i and ATP levels over time in a model of the rheostat pathway including ATPase activity. (**c**) Detail of P_i and ATP levels over time in the model of the stoichiometric pathway shown in **a**. (**d**) Detail of P_i and ATP levels over time in the model of the rheostat pathway shown in **b**. The initial conditions contained 4 mM P_i, and ATP hydrolysis was held constant. Modeling parameters are provided in **Supplementary Table 5**.

branch also produces NADPH, but first converts G3P into 1,3-bisphosphoglycerate (1,3-BPG), which is followed by PGK-catalyzed conversion to 3PG along with production of ATP. Therefore, the mGapDH–PGK branch produces an additional equivalent of ATP compared to the GapN-only branch.

The relative flow through the ATP-generating branch of the rheostat is controlled by free P_i, which acts as a proxy for the amount of ATP hydrolyzed to ADP and P_i. The function of the rheostat is easiest to see in the simplest case, in which no exogenous P_i is added to the reaction (**Fig. 1c**). In this case there is initially no free P_i, and there can be no flux through the phosphorylating mGapDH . Thus, in the absence of P_i, all the flux passes through the GapN branch. Only when ATP is hydrolyzed to ADP and P_i can the phosphorylating branch be used. Therefore, the rheostat responds to the depletion of ATP and acts to restore ATP by using the phosphorylating mGapDH branch.

To explore the effectiveness of this design, we used COPASI to construct a computer model of the overall pathways with and without the rheostat, including in the model a low level of ATPase activity (**Fig. 3**). As expected, flux through the stoichiometric pathway, relying only on GapN, gradually decreases when any amount of ATP hydrolysis is introduced, much like the results we observed experimentally. When this pathway is supplemented with mGapDH and PGK to complete the molecular rheostat, the reaction reaches a steady state and proceeds to completion. In this model, the molecular rheostat reaches a steady state any time the flux through mGapDH and PGK is greater than the ATPase activity being introduced. Thus, the regulatory node should be able to operate at a wide range of ATPase activities, with no need to perfectly tune and match the system to the specific amount of ATP hydrolysis, for the system to reach a steady state. The autoregulatory behavior of the rheostat is a key feature for designing robust, self-sustaining *in vitro* enzymatic pathways.

Engineering mGapDH

To implement our molecular rheostat module, we needed to engineer a GapDH enzyme that would efficiently use $NADP^+$ rather than NAD^+. We started with the *Geobacillus stearothermophilus* GapDH (*Gs*Gap), which strongly prefers NAD^+ over $NADP^+$. Although the cofactor specificity of *Gs*Gap has been adjusted before by sequence-based design[24], the resulting variant only slightly preferred $NADP^+$ over NAD^+. To generate a mutant *Gs*Gap with higher cofactor specificity for $NADP^+$, we re-examined the *Gs*Gap crystal structure[24] and introduced basic residues into the loop region proximal to the 2OH of NAD^+, which might help stabilize binding of the 2′ phosphate in $NADP^+$ (**Supplementary Fig. 2**). We made a series of mutations to residues D32, L33 and T34. The kinetics and specificity of the most selective enzyme, a D32A L33R T34K triple mutant (herein referred to as mGapDH), are shown in **Supplementary Table 2**. The wild-type *Gs*Gap enzyme strongly preferred NAD^+, but the triple-mutant mGapDH had a 30-fold preference for $NADP^+$ over NAD^+ (as measured by k_{cat}/K_m).

Isobutanol production with the molecular rheostat

To implement the molecular rheostat for the production of isobutanol from glucose, we added the two enzymes, mGapDH and PGK, to the optimized stoichiometric reaction containing GapN. To ensure sufficient ATP production through the molecular rheostat, the units of mGapDH- and PGK-specific activity in the reaction were set at an order of magnitude greater than the aggregate ATPase activity in the reaction. We set up side-by-side reactions with and without the molecular rheostat and assayed for isobutanol production, residual glucose and ATP over a 72-h time course (**Fig. 4**). The reaction with the molecular rheostat produced 24.1 ± 1.8 g/L of isobutanol at 91.5% of the theoretical yield with a maximum productivity of 1.4 ± 0.3 g/L/h. To our knowledge, these titers and yields of isobutanol production are higher than those of any published *in vivo* systems that do not implement complex *in situ* isobutanol removal.

The molecular rheostat performed as expected, maintaining a higher ATP concentration than the stoichiometrically balanced reaction. As shown in **Figure 4**, the rheostat reaction held an ATP steady state concentration at around 600 μM for 48 h. ATP levels dropped only after glucose consumption ended, and, with it, the ability to generate additional ATP. By contrast, the ATP concentration in the stoichiometric reaction steadily decreased throughout the entire run. Over the first 48 h of both reactions, there was a good correlation between the concentration of ATP in the reaction and isobutanol production (**Fig. 4a**,**c**). To further test the importance of the rheostat system for isobutanol production, we omitted specific rheostat components from the reaction system. As shown in **Figure 4d**, when either the GapN branch or the mGapDH–PGK branch was left out, production of isobutanol was drastically reduced compared to the full molecular rheostat system. Thus, the rheostat system was critical for obtaining high-level isobutanol production.

Enzyme stability limits production

Although the system containing the molecular rheostat produced a self-sustaining reaction and maintained a steady state concentration of ATP for the first 48 h, the reaction completely stopped after 72 h. In the reaction with the molecular rheostat, we noticed a precipitate that began to form after 24 h, which coincided with a decrease in isobutanol production. These results suggested that some of the enzymes were denaturing over time, possibly because of increasing isobutanol concentrations.

To determine the stability of each system component to isobutanol, each enzyme and cofactor in the pathway was tested for stability in 0%, 4% and 8% (saturating) isobutanol (**Supplementary**

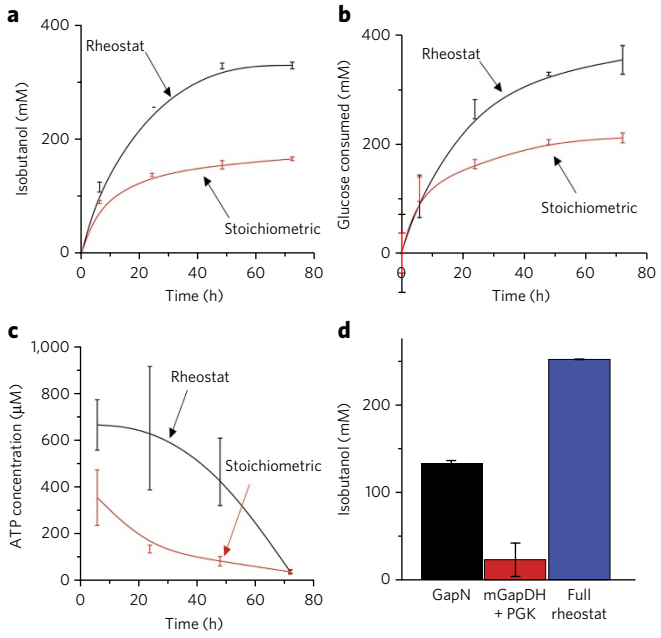

Figure 4 | Final production of isobutanol. (**a**) Time course of isobutanol production with (black) and without (red) the rheostat. (**b**) Time course of glucose consumption with (black) and without (red) the rheostat. (**c**) Time course of ATP concentration in the reaction with (black) and without (red) the rheostat. (**d**) Histogram of isobutanol production after 24 h using GapN only; mGapDH and PGK only; or the full rheostat system (GapN, mGapDH and PGK). Error bars represent the s.d. of biological replicates performed in triplicate.

Fig. 3). Hex, GapN, mGapDH and IlvC were found to be the most susceptible to isobutanol inactivation. A more detailed investigation of the susceptibility of GapN and KivD to isobutanol inactivation revealed nearly complete inactivation after 24 h in 2.5% isobutanol (**Supplementary Fig. 4**). These results rapidly identified a handful of enzymes that are high-priority targets for improving their stability to increase the overall sustainability of the system.

DISCUSSION

Our results provide another demonstration of an *in vitro* cofactor regulatory system that adds to the many benefits of a cell-free synthetic biochemistry approach. Because cell-free synthetic biochemistry systems are well defined, we can readily employ modeling to test design effectiveness and identify key parameters. Once designed, the modeling results can be rapidly implemented and further optimized experimentally. Moreover, ready access to the relatively small number of system components (compared to cells or cell lysates) of the reaction allows for the rapid isolation of problems. For example, we could quickly identify ATPase contamination and seek to remedy it. Moreover, we could easily identify the enzymes that will need to be stabilized for future improvements.

Synthetic biochemistry systems that do not rely on perfect stoichiometry should run longer, and be more flexible, than those with strict stoichiometric requirements. The molecular rheostat can be considered a form of metabolite proofreading, as it corrects for unwanted ATP hydrolysis[23]. Previously, we described a complementary 'molecular purge valve' that regulates the production and consumption of $NAD(P)^+$/NAD(P)H[16]. Together with the 'molecular rheostat' that regulates ATP described here, these novel *in vitro* tools can enable the design of self-sustaining *in vitro* pathways for a myriad of bio-based products that require balancing both $NAD(P)^+$/NAD(P)H and ATP individually or at the same time. The development of self-regulatory nodes that can control ATP and $NAD(P)^+$/NAD(P)H puts us closer to realizing the potential of industrial cell-free enzymatic synthesis. A major practical limitation for commercial feasibility remains the procurement of enzymes that are sufficiently stable to warrant the added initial investment required to produce them.

Received 6 December 2016; accepted 11 May 2017;
published online 3 July 2017

METHODS

Methods, including statements of data availability and any associated accession codes and references, are available in the online version of the paper.

References

1. Cameron, D.E., Bashor, C.J. & Collins, J.J. A brief history of synthetic biology. *Nat. Rev. Microbiol.* **12**, 381–390 (2014).
2. Kwok, R. Five hard truths for synthetic biology. *Nature* **463**, 288–290 (2010).
3. Zhang, Y.-H.P. Simpler is better: high-yield and potential low-cost biofuels production through cell-free synthetic pathway biotransformation (SyPaB). *ACS Catal.* **1**, 998–1009 (2011).
4. Zhang, Y.-H.P. Production of biocommodities and bioelectricity by cell-free synthetic enzymatic pathway biotransformations: challenges and opportunities. *Biotechnol. Bioeng.* **105**, 663–677 (2010).
5. Schultheisz, H.L., Szymczyna, B.R., Scott, L.G. & Williamson, J.R. Pathway engineered enzymatic *de novo* purine nucleotide synthesis. *ACS Chem. Biol.* **3**, 499–511 (2008).
6. Schultheisz, H.L., Szymczyna, B.R., Scott, L.G. & Williamson, J.R. Enzymatic *de novo* pyrimidine nucleotide synthesis. *J. Am. Chem. Soc.* **133**, 297–304 (2011).
7. Rollin, J.A., Tam, T.K. & Zhang, Y.-H.P. New biotechnology paradigm: cell-free biosystems for biomanufacturing. *Green Chem.* **15**, 1708–1719 (2013).
8. Krutsakorn, B. *et al.* In vitro production of *n*-butanol from glucose. *Metab. Eng.* **20**, 84–91 (2013).
9. Hodgman, C.E. & Jewett, M.C. Cell-free synthetic biology: thinking outside the cell. *Metab. Eng.* **14**, 261–269 (2012).
10. Zhu, Z., Kin Tam, T., Sun, F., You, C. & Percival Zhang, Y.-H. A high-energy-density sugar biobattery based on a synthetic enzymatic pathway. *Nat. Commun.* **5**, 3026 (2014).
11. Zhang, Y.-H.P., Evans, B.R., Mielenz, J.R., Hopkins, R.C. & Adams, M.W.W. High-yield hydrogen production from starch and water by a synthetic enzymatic pathway. *PLoS One* **2**, e456 (2007).
12. Ye, X. *et al.* Spontaneous high-yield production of hydrogen from cellulosic materials and water catalyzed by enzyme cocktails. *ChemSusChem* **2**, 149–152 (2009).
13. Welch, P. & Scopes, R.K. Studies on cell-free metabolism: ethanol production by a yeast glycolytic system reconstituted from purified enzymes. *J. Biotechnol.* **2**, 257–273 (1985).
14. Korman, T.P. *et al.* A synthetic biochemistry system for the *in vitro* production of isoprene from glycolysis intermediates. *Protein Sci.* **23**, 576–585 (2014).
15. Guterl, J.-K. *et al.* Cell-free metabolic engineering: production of chemicals by minimized reaction cascades. *ChemSusChem* **5**, 2165–2172 (2012).
16. Opgenorth, P.H., Korman, T.P. & Bowie, J.U. A synthetic biochemistry module for production of bio-based chemicals from glucose. *Nat. Chem. Biol.* **12**, 393–395 (2016).
17. Opgenorth, P.H., Korman, T.P. & Bowie, J.U. A synthetic biochemistry molecular purge valve module that maintains redox balance. *Nat. Commun.* **5**, 4113 (2014).
18. Atsumi, S. *et al.* Evolution, genomic analysis, and reconstruction of isobutanol tolerance in *Escherichia coli*. *Mol. Syst. Biol.* **6**, 449 (2010).
19. Atsumi, S. *et al.* Engineering the isobutanol biosynthetic pathway in *Escherichia coli* by comparison of three aldehyde reductase/alcohol dehydrogenase genes. *Appl. Microbiol. Biotechnol.* **85**, 651–657 (2010).
20. Li, X., Shen, C.R. & Liao, J.C. Isobutanol production as an alternative metabolic sink to rescue the growth deficiency of the glycogen mutant of *Synechococcus elongatus* PCC 7942. *Photosynth. Res.* **120**, 301–310 (2014).
21. Atsumi, S., Hanai, T. & Liao, J.C. Non-fermentative pathways for synthesis of branched-chain higher alcohols as biofuels. *Nature* **451**, 86–89 (2008).

22. Valverde, F., Losada, M. & Serrano, A. Engineering a central metabolic pathway: glycolysis with no net phosphorylation in an *Escherichia coli* gap mutant complemented with a plant GapN gene. *FEBS Lett.* **449**, 153–158 (1999).
23. Van Schaftingen, E. *et al.* Metabolite proofreading, a neglected aspect of intermediary metabolism. *J. Inherit. Metab. Dis.* **36**, 427–434 (2013).
24. Didierjean, C. *et al.* Crystal structure of two ternary complexes of phosphorylating glyceraldehyde-3-phosphate dehydrogenase from *Bacillus stearothermophilus* with NAD and D-glyceraldehyde 3-phosphate. *J. Biol. Chem.* **278**, 12968–12976 (2003).

Acknowledgments

The authors thank members of the Bowie lab for helpful comments. This work was supported by DOE grants DE-FC02-02ER63421 and DE-AR0000556 to J.U.B.

Author contributions

P.H.O., T.P.K. and J.U.B. contributed to the system design. P.H.O., T.P.K., L.I. and J.U.B. contributed to the design of experiments and data analysis. P.O., L.I. and T.K. performed the experiments. P.H.O., T.P.K. and J.U.B. wrote the paper.

Competing financial interests

The authors declare competing financial interests: details accompany the online version of the paper.

Additional information

Any supplementary information, chemical compound information and source data are available in the online version of the paper. Reprints and permissions information is available online at http://www.nature.com/reprints/index.html. Publisher's note: Springer Nature remains neutral with regard to jurisdictional claims in published maps and institutional affiliations. Correspondence and requests for materials should be addressed to J.U.B.

ONLINE METHODS

Materials. Miller LB media or Miller LB-agar (BD Difco) was used for growth of bacterial strains in liquid or solid media. *E. coli* BL21Gold(DE3) [B, F-, *ompT, hsdS*$_{B,}$ (r_B–,m_B–), *dcm*+,*Tet*^{r},*gal*λ,(DE3) *endA Hte*] (Agilent) was used as a host for both cloning and expression of recombinant proteins using pET vectors. *E. coli* TOP10(DE3) (F- mcrA Δ(mrr-hsdRMS-mcrBC) ϕ80lacZΔM15 ΔlacX74 nupG recA1 araD139 Δ(ara-leu)7697 galE15 galK16 rpsL(Str^R) endA1 λ$^-$) was used for expression of recombinant proteins from the pBAD/p15A vector. Plasmids pET28a(+) and pET22b(+) were purchased from Novagen. HotStart Taq Mastermix (Denville) was used for gene amplification from genomic or plasmid DNA. *Phusion* DNA polymerase (Finnizymes), Taq DNA ligase (MCLab), and T5 Exonuclease (Epicenter) were purchased separately and used to make the assembly master mix (AMM) used for cloning. ATP, pyruvate, and NAD(P)$^+$ were obtained from Sigma.

Plasmid construction. The expression plasmids for the enzymes were constructed from the pET28a plasmid backbone using the Nde1 and Sac1 cut sites to produce constructs with an N-terminal 6×His tag for purification. Primers used for cloning are listed in **Supplementary Table 7**.

Enzyme expression and purification. Enzymes were expressed and purified as described previously[14,17]. All enzyme activities and purification conditions are listed in **Supplementary Table 2**.

CoPASI modeling. CoPASI v4.16 was downloaded from http://copasi.org/. For simulation and analysis of the combined isobutanol pathways designed in this study, K_m and k_{cat} values were obtained from the BRENDA database (**Supplementary Table 6**), and rate equations (**Supplementary Note**) were derived based on descriptions of yeast metabolism. A time-course task was run with a time scale of 90,000 s, and ATPase was set at 0.01 s^{-1}. The ATP rheostat was modeled under the same conditions, with the addition of mGapDH and PGK.

Enzyme activity and optimization. The enzymes were assayed in 200-µl reactions using a standard buffer consisting of 50 mM Tris buffer pH 7.5, 5 mM $MgCl_2$, 0.25 mM TPP and 5 mM KCl, which mirrors the final reaction conditions. The individual assays components, including the coupling enzymes, metabolites and substrates are given in **Supplementary Table 3**. The activity of NAD(P)H-producing or consuming reactions were monitored at 340 nm with a Molecular Dynamics plate reader. The activity of ATP-consuming enzymes were monitored using a coupled assay and NADP$^+$ at 340 nm.

ATPase assays of the enzymes were tested in a coupled enzyme assay with 5 mM PEP, 1 mM ATP, 1 µl PK/LDH, 0.25 mM NADH and started upon the addition of the given enzyme. The ATPase activity was calculated by the decrease in NADH concentration over 2 h, determined by absorbance changes at 340 nm, using an extinction coefficient of 6.2 mM^{-1} cm^{-1}.

The stoichiometric reaction system was initially set up with largely arbitrary enzyme concentrations, except that all the enzyme-specific activities were set substantially higher than that of hexokinase. The isobutanol concentration produced after 18 h using this initial system served as a baseline. We then systematically increased two-fold or decreased five-fold each enzyme individually, holding the other enzymes constant, and assayed the isobutanol production after 18 h. Increasing AlsS and IlvC enzymes concentrations and decreasing the KivD concentration were found to improve production from the baseline. We therefore increased AlsS and IlvC enzymes two-fold and decreased the KivD enzyme five-fold in the final system, which increased isobutanol production. No further optimization was performed.

Final isobutanol reaction conditions and analysis. The optimized self-sustaining reaction for the biotransformation glucose to isobutanol was composed of 50 mM Tris pH 7.5, 5 mM $MgCl_2$, 5 mM KCl, 2 mM NADP$^+$, 4 mM ATP, 1 mM glutathione, 0.25 mM TPP, 0.25 mM $MnCl_2$, 4 mM P_i, 0.25 mM 1,3-BPG, and 660 mM glucose in a final reaction volume of 200 µl. The enzyme concentrations are listed in **Supplementary Table 4**. The reactions were initiated with the addition of glucose, which was left out of the initial mixture. All reactions were performed in triplicate at room temperature.

To assay for isobutanol, the reactions were extracted with 0.3 ml hexanes. 1 µl of the hexane layer was applied to a 0.25 micron HP-INNOWax column using a HP 5890 Series II gas chromatogram. The gas chromatography method used an injection temperature that was held at 50 °C for 5 min, before it was increased to 275 °C over 35 min. The peak intensities were compared to an authentic standard to assess concentrations.

Data availability. The data that support the findings of this study are available from the authors upon reasonable request. Source data files for **Figures 2–4** are available online.